LA-UR-74-1796

CONF-741221--2

TITLE: QUANTITATIVE DETERMINATION OF FISSION PRODUCTS IN IRRADIATED FUEL PINS USING NONDESTRUCTIVE GAMMA SCANNING

AUTHOR(S): J. R. Phillips, G. R. Waterbury, N. E. Vanderborgh, and T. K. Marshall

SUBMITTED TO: Third Inter-American Meeting on Radiochemistry, São Paulo, Brazil, December 2-6, 1974.

MASTER

By acceptance of this article for publication, the publisher recognizes the Government's (license) rights in any copyright and the Government and its authorized representatives have unrestricted right to reproduce in whole or in part said article under any copyright secured by the publisher.

The Los Alamos Scientific Laboratory requests that the publisher identify this article as work performed under the auspices of the U. S. Atomic Energy Commission.

los alamos
scientific laboratory
of the University of California
LOS ALAMOS, NEW MEXICO 87544

NOTICE
This report was prepared as an account of work sponsored by the United States Government. Neither the United States nor the United States Atomic Energy Commission, nor any of their employees, nor any of their contractors, subcontractors, or their employees, makes any warranty, express or implied, or assumes any legal liability or responsibility for the accuracy, completeness or usefulness of any information, apparatus, product or process disclosed, or represents that its use would not infringe privately owned rights.

Form No. 836
St. No. 2629
1/73

UNITED STATES
ATOMIC ENERGY COMMISSION
CONTRACT W-7405-ENG. 36

LA-UR-74-1796

Quantitative Determination of Fission Products in Irradiated Fuel Pins Using Nondestructive Gamma Scanning*

J. R. Phillips, G. R. Waterbury
N. E. Vanderborgh, T. K. Marshall

Los Alamos Scientific Laboratory
University of California
Los Alamos, New Mexico

ABSTRACT

A computer-controlled gamma scanning system was applied to the nondestructive determination of fission products in irradiated uranium-plutonium carbide and oxide fuel pins. The quantitative determinations were made possible by a detailed calibration of the gamma scanning system including: measurement of the effective collimating slit, detector surface response functions, and the development of a computer code for simulation of various source geometries. Following the nondestructive gamma scanning examinations of the irradiated fuel materials, the samples were dissolved remotely, and analyzed independently by well-proven radiochemical methods. The gamma scanning results differed by an average of 3.2% and 3.7% for three fission products (^{106}Ru-^{106}Rh, ^{137}Cs, and ^{144}Ce-^{144}Pr) in three (U, Pu) carbide samples and three UO_2-PuO_2 samples, respectively. These data indicate that precision gamma scanning can be applied to the nondestructive determination of fission products in irradiated (U, Pu) carbide and oxide fuel pins.

*Performed for the Division of Reactor Research and Development of the United States Atomic Energy Commission.

INTRODUCTION

Precision gamma scanning is a very useful nondestructive technique for measuring the relative isotopic distributions of activation and fission products as a function of precise axial and radial position in irradiated fuel pins. These isotopic distributions provide valuable information required for the determination of the migration mechanisms of specific fission products, the calculation of the relative burnup profiles, the correlation of axial and radial temperature gradients, and the measurement of fuel swelling and redistribution.[1, 2, 3, 4]

Recent advances in data interpretation of this nondestructive technique now permit quantitative measurements of activation and fission products, thereby, adding another important dimension to precision gamma scanning. The nondestructive quantitative determination of isotopes in irradiated fuel pins can provide data for the determination of the absolute mass transfer mechanisms of fission products, the measurement of fast and thermal neutron flux components of the irradiation exposure, the measurement of burnup and burnup profiles, and other important factors concerning the chemical and physical characteristics of the irradiated fuel materials.

There are two basic approaches to quantitative gamma scanning: the first approach involves the direct comparison of irradiated standards and the unknown fuel materials, and the second approach involves the extensive calibration of the gamma scanning system and the complete characterization of the fuel materials. The Los Alamos Scientific Laboratory (LASL) gamma scanning facility examines approximately 150 experimental fuel pins annually for the Liquid Metal Fast Breeder Reactor (LMFBR) program representing many different fuel materials, fuel densities, cladding materials, irradiation exposures, and decay periods. Therefore, we selected the second approach because of the impossibility of maintaining an adequate inventory of irradiated standards to simulate the large number of experimental fuel pins examined at LASL.

The complete calibration of the LASL gamma scanning system includes: the calibration of the scanning mechanism to ensure the precise positioning of the fuel pin, the experimental measurement of the effective collimating slit areas, and the determination of the efficiency surface response functions of

the detector assembly. These data are combined with the appropriate source factors including: subtended solid angle, fuel volume segment, fuel and cladding materials, and other source parameters to obtain the total response function for the specific gamma-emitting isotope for each fuel pin examined. The total response function relates the number of full-energy gamma rays absorbed by the detection assembly to the total number of fission or activation products present in the volume segment of the irradiated fuel viewed by the detector.

This unique technique has been applied successfully to the examination of irradiated (U, Pu)C fuel segments for the quantitative measurement of ^{106}Ru-^{106}Rh, ^{137}Cs, and ^{144}Ce-^{144}Pr. Also, the method was used to determine the quantities of ^{106}Ru-^{106}Rh, ^{137}Cs, ^{144}Ce-^{144}Pr, and ^{95}Zr in UO_2-PuO_2 fuel segments. The UO_2-PuO_2 samples were more difficult to process because of the significant axial and radial migration of the fission products within the fuel matrices.

EXPERIMENTAL

The LASL gamma scanning system consists of essentially four basic segments: the precision scanning mechanism, the gamma-ray beam collimation assembly, the anticoincidence detector assembly, and the computer-controlled data acquisition unit (Fig. 1).[4] The scanning mechanism has five degrees of motion: X (left-right), Y (in-out), Z (up-down), tilt, and rotation. Each motion is controlled by precision stepping motors coupled to absolute-position shaft encoders with binary-coded decimal readout. The precision associated with the specific motions are ±0.025 mm for the X, Y, Z, and tilt motions, and ±0.035 radians for the rotation motion. The two principal motions in quantitative gamma scanning, X and Z, were calibrated to determine their spatial accuracy using two accurately measured ^{60}Co sources separated by a precisely measured aluminum rod with all the measurements traceable to length standards of the National Bureau of Standards (NBS). The precise calibration of the scanning mechanism was one of the most critical steps because of the requirement of precise measurement of fission and activation product distributions axially and radially in the irradiated fuel pin.

The collimating slit assembly consists of a primary collimator located in the hot cell wall next to the fuel pin and two secondary beam-scraping collimators for the precise definition of the

gamma-ray beam. The primary collimator is constructed of a high-density tungsten alloy insert surrounded with low-gamma-activity lead. The tungsten alloy has a linear gamma attenuation coefficient 1.45 times as large as lead, thereby resulting in a better gamma-ray beam defining material. The secondary collimators are constructed of lead and are spaced at specified positions between the detector and primary collimator to optimize reduction of scattering effects as well as to define precisely the gamma-ray beam striking the detector's surface.

The collimators were inspected using 22 MeV x-rays to ensure uniformity of material and precision of construction.[5] Following the radiographic inspection, the collimators were mechanically inspected to determine possible variations in the slit widths within each collimator with a precision of ±0.0005 mm. Once the collimators passed these two examinations, they were placed in the collimation assembly.

The effective collimating slit areas were measured at various positions along the principal axis of the gamma-ray beam by using an irradiated fuel pin as a high-intensity source to expose x-ray film. The optical densities of the resulting images were measured using a precision microphotometer and the densities were converted to intensities as a function of precise position in the X and Z directions. The resulting experimentally measured images were compared to the theoretical images obtained from a computer code for simulating various collimator arrangements.[4]

The theoretical and experimental images in the Z-direction (up-down) were calculationally simulated using an analytical function consisting of a Gaussian term plus a background term by means of a least squares routine.[6] The widths of the calculated functions were measured at a standard height, M/e, (M = maximum height of the function and e = base of the Naperian logarithms). The calculated widths of the theoretical images at M/e for collimators ranging from 0.508 mm (0.020 in.) to 0.610 mm (0.024 in.) are presented in Table I.

The experimental width of the gamma-ray beam was measured at several positions along the beam's path to determine the effective collimating slit area. Table II shows the results of three measurements obtained at the detector's surface.

The experimentally determined value of 9.16 ± 0.13 mm corresponds to the value obtained from the theoretical slit 0.559 mm (0.0220 in.) of 9.164 mm. Similar measurements were performed in the X-direction (left-right) resulting in a theoretical model of the effective collimating slit area at the detector's surface. The physical measurement of the collimating slit indicated that the slit was 0.508 mm (0.0200 in.) which differed by 0.051 mm (0.0020 in.) from that measured experimentally. The effective slit 0.559 mm (0.0220 in.) was used for the calculation of the collimating assembly.

The detector's area is 1274 mm^2 and the gamma-ray beam area is only 237 mm^2 at the detector's surface, resulting in only 18% of the detector's surface being exposed to the gamma-ray beam. This is illustrated in Fig. 2 where the simulated gamma-ray beam image is superimposed on the surface of the detector. The density of the beam's image varies over the exposed area in the X- and Z- directions. The variation in the Z-direction was represented by a Gaussian function as discussed previously.

If the detector's surface response function were uniform over the entire detector's surface, the fact that only a small area (18% of the total area) of the detector's surface was exposed to the gamma-ray beam would be insignificant. However, the surface response functions vary significantly with gamma photon energy as well as with the relative surface positions.[7] The relative efficiency for a specific gamma photon energy can vary by a factor of 3.2 due to changes in the depth of the intrinsic region of the coaxial Ge(Li) detector. The relative surface response function for the 661.6 keV gamma-ray energy (^{137}Cs) is presented in Fig. 3 as an isometric projection to illustrate the relative magnitude of the variations over the detector's surface. The surface response function was measured experimentally using a precisely collimated gamma-ray beam from International Atomic Energy Agency (IAEA) certified sources.

When the variations in the gamma-ray efficiency as a function of surface position are combined with the nonuniform gamma-ray beam, the precise alignment of the collimated gamma-ray beam with respect to the detector's surface becomes one of the most critical steps in the entire calibration procedure. Any variation of the gamma-ray beam's position on the detector's surface can seriously distort the total response function for the specific source. Therefore, the detection assembly is mounted on a mechanism to allow the precise positioning within ±0.25 mm.

Up to this point we have considered the scanning mechanism, the collimation assembly, and the detector's response functions, but have not considered the gamma-ray source and the factors influencing its gamma-ray strength. A computer program was developed to simulate any fuel pin arrangement that might be examined. The code randomly selects a specified number of source points in the three-dimensional volume segment of the fuel pin defined by the effective collimating slits. The attenuation effects of the fuel material, thermal bonding, cladding material, and structural material and subtended solid angle are considered to determine the fraction of each source point's activity impinging the exposed surface of the detector. The surface response functions determined above are used to calculate the absorption efficiency of the gamma photon to measure the total response for the specific source point. This calculation is performed for all of the specified source points and the results appropriately weighted to determine the total response functions for the volume segment, which can be related to the total number of that particular isotope.

The basic factors to be considered in the source are the attenuating materials and densities, spatial location of materials, and the radial isotopic distributions of the fission products. Differences in the radial isotopic distributions can result in significant errors for certain isotopes. It is necessary, therefore, to determine the radial isotopic distributions prior to the quantitative determination by scanning the fuel pin diametrally at two or more angular orientations.[8] The diametral distributions are unfolded using bi-cubic spline functions for interpolation, resulting in the two-dimensional radial distributions for each specified isotope.

The total response function for a particular isotope is dependent on: the fuel material, cladding materials, source geometry factors, and radial distribution for the specific irradiated fuel pin as well as the effective collimating slit area and the detector's surface response function.[4] These factors were calculated for a set of three (U, Pu)C fuel segments and a set of three UO_2, PuO_2 fuel segments for determining the precision of this unique nondestructive method.

DISCUSSION AND RESULTS

Three sections, 12 mm long and about 6 mm in diameter of irradiated (U, Pu)C fuel pins with burnups of approximately 9.5 at. % were nondestructively gamma scanned to determine the quantities of ^{106}Ru- ^{106}Rh, ^{137}Cs, and ^{144}Ce- ^{144}Pr. Following this examination the three sections were dissolved and analyzed using well-proven radiochemical methods. The comparison of the nondestructive gamma scanning results with the destructive radiochemical results are presented in Table III. The absolute average deviation for all three fission products was 3.2% for the three (U, Pu)C sections.

Three irradiated UO_2-PuO_2 fuel sections 12-mm long, 5.6 mm in diameter were similarly examined for ^{106}Ru- ^{106}Rh, ^{137}Cs, ^{144}Ce-^{144}Pr, and ^{95}Zr to determine the applicability of this nondestructive technique to oxide fuels. The results for these four fission products in the three UO_2-PuO_2 fuel sections are presented in Table IV.

The second ^{106}Ru- ^{106}Rh result of the gamma scanning data ($1.34 \pm 0.03 \times 10^{18}$ atoms) was significantly different (40.1%) from the corresponding radiochemical result ($9.55 \pm 0.12 \times 10^{17}$ atoms). This difference is substantially above that associated with possible statistical variations. This particular fuel section was scanned diametrally at two different angular orientations to determine the radial isotopic distributions of the fission products.[8] The radial distribution of ^{106}Ru- ^{106}Rh indicated

that a significant amount (about 20% of the total activity) of the isotope was deposited around the central void of the oxide fuel probably in the form of metallic ingots. It is quite possible that the ^{106}Ru- ^{106}Rh was dislodged and lost during the removal of the sample from the scanning container or during the transfer to the dissolution container. The relative full-energy peak activities were checked to determine the relative activities of the 662 keV ^{106}Ru- ^{106}Rh peak with respect to the 661.6 keV ^{137}Cs and 695 keV ^{144}Ce- ^{144}Pr gamma-ray peaks. The relative activities indicated that about 25% of the ^{106}Ru- ^{106}Rh activity was physically lost prior to the radiochemical analysis. The possible loss of sample material is eliminated when nondestructive gamma scanning is used to examine the sample. The sample's integrity is maintained allowing the sample to be re-analyzed to check the results if necessary.

The ^{106}Ru- ^{106}Rh, ^{137}Cs, and ^{144}Ce- ^{144}Pr gamma scanning results compare very well with the radiochemical results with average differences of 4.3%, 4.0%, and 2.9%, respectively. The ^{95}Zr results show a constant bias of about 9.3%, with the gamma scanning results being lower than the radiochemical results. The surface response function for the 661.6 keV ^{137}Cs isotope was used to represent the response functions for all four isotopes: 622 keV ^{106}Ru- ^{106}Rh, 661.6 keV ^{137}Cs, 695 keV ^{144}Ce- ^{144}Pr, and 724 keV ^{95}Zr. The 661.6 keV surface response function was interpolated for each of the other gamma-ray energies by considering the appropriate linear absorption coefficients. This method of interpolation was satisfactory for the gamma-ray energies close to the starting energy of 661.6 keV, in particular, 622 keV ^{106}Ru- ^{106}Rh and 695 keV ^{144}Ce- ^{144}Pr. However, as the energy difference increases a more refined method of interpolation may be required. The fraction of gamma photons absorbed in the germanium by Compton scattering increases while the absorption due to photoelectric interaction decreases as the energy of the photon increases.

The best method for determining the surface response function for a specific gamma-ray energy would be to determine experimentally the function using a precisely collimated gamma-ray beam. We have determined the surface response functions for the detector over the energy range of 60-1800 keV by using IAEA certified sources: 59.6 keV (^{241}Am), 122 and 136.3 keV (^{57}Co), 511 keV (^{22}Na), 661.6 keV (^{137}Cs), 834.5 keV (^{54}Mn), 898 keV (^{88}Y), 1173.2 and 1332.5 keV (^{60}Co), and 1836.1 keV (^{88}Y).[4]

The examination of each of the above 12-mm fuel sections required about 2 man-days for the gamma scanning and data analysis. To examine a complete fuel pin with a 350-mm fuel column would require about 7 man-days. Comparable destructive analysis of the fuel pin including: sectioning in 12-mm segments, complete dissolution of the fuel and cladding material, and the radiochemical analysis of the samples, would require about 40 man-days. The destructive analysis still would not result in the spatial discrimination (0.5 mm) which is routinely provided by the gamma scanning technique.

There are several obvious applications of this technique for quantitative determination of fission products within the fuel material. For example, the burnup can be determined at any axial position using the total ^{137}Cs in the fuel sections. This was done on three (U, Pu) C sections. The relative burnup values (Table V) agree very well between the two methods, gamma scanning and mass spectrometry, as indicated by the normalized values. This nondestructive method is not as precise as the mass spectrometric technique, but the gamma scanning technique allows the determination of burnup during an interim examination without disturbing the fuel pin's integrity.

The quantitiative measurement of volatile fission products would permit the determination of absolute mass transfer mechanisms. Often times ^{134}Cs and ^{137}Cs migrates axially in UO_2-PuO_2 fuel pins, depositing in inter-pellet gaps at the insulator-fuel interface, or on structural material. This gamma scanning technique would provide the necessary information as to the quantities of ^{134}Cs and ^{137}Cs deposited at any specific location. This would especially be important for investigating the effect of possible cladding attack by the cesium isotopes as a function of cesium concentration.

CONCLUSIONS

The quantitative determination of fission products within irradiated (U, Pu)C and UO_2-PuO_2 fuel pins has been illustrated without the requirement of using irradiated standards. The gamma scanning system was extensively calibrated: the scanning mechanism for the precise positioning of the fuel pin, the effective collimating slit for defining the volume segment of the fuel pin, the surface response functions of the detection assembly, and the total response functions of various simulated sources. The quantitative determinations of the three fission products ^{106}Ru- ^{106}Rh, ^{137}Cs, and ^{144}Ce- ^{144}Pr in three carbide and three oxide fuel sections were accomplished with precisions of 3.2% and 4.3% for the carbide and oxide samples, respectively. The quantitative determination of ^{95}Zr in the three UO_2-PuO_2 sections showed a negative bias of 9.3% which may be related to the method of interpolation of the surface response functions.

ACKNOWLEDGEMENTS

The authors wish to acknowledge the valuable assistance of J. R. Netuschil in processing the raw data and J. N. Quintana in the data collection. The fuel dissolutions were performed by J. W. Dahlby, with J. Bubernak analyzing the radiochemical samples. The research was performed under the auspices of the Division of Reactor Research and Development of the United States Atomic Energy Commission.

REFERENCES

1. C. Engleman, C. Brebant, J. Grosset, J. Monier, E. Roussel, "Potentialities of Gamma Spectrometry in Nondestructive Measurements on Fuel Elements," STI/PUB/105, Vol. II, pp 139-149 (1965).
2. N. C. Rasmussen, "The Nondestructive Analysis of Spent Reactor Fuel by Gamma-Ray Spectrometry," USAEC report WASH-1076, pp 130-137 (1967).
3. D. M. Holm, W. M. Sanders, J. L. Parker, H. D. Cowan, "Examination of Fast Reactor Fuel Elements with a Ge(Li) Anticoincidence Gamma-Ray Spectrometer," Proc. 16th Conf. Remote Syst. Technol., pp 228-242 (1969).
4. J. R. Phillips, "New Techniques in Precision Gamma Scanning; Application to Fast-Breeder Reactor Fuel Pins," Los Alamos Scientific Laboratory report LA-5260-T (July 1973).
5. D. E. Elliot, J. F. Torbert, "Radiographic Inspection of Irradiated Fuel Elements Using 22 MeV Betatron," Proc. 16th Conf. Remote Syst. Technol., pp 222-225 (1969).
6. R. H. Moore, R. K. Zeigler, "Solution of the General Least Squares Problem with Special Reference to High-Speed Computers," Los Alamos Scientific Laboratory report LA-2367 (1959).
7. H. L. Malm, IEEE Trans. on Nucl. Sci. NS, 13(3) p 285 (1966).
8. B. K. Barnes, J. R. Phillips, "TWODIM: A Computer Code for Unfolding Diametral Gamma-Ray Scans on Reactor Fuel Elements," Los Alamos Scientific Laboratory report LA-4676 (1971).

TABLE I

Calculated Widths of Theoretical Slits

Theoretical Slit Width	Theoretical Width at Detector's Surface	Least Squares Width[a]
0.508 mm (0.0200 in.)	8.380 mm	8.297 mm
0.533 mm (0.0210 in.)	8.470 mm	8.598 mm
0.546 mm (0.0215 in.)	8.730 mm	8.848 mm
0.559 mm (0.0220 in.)	9.385 mm	9.164 mm
0.572 mm (0.0225 in.)	9.505 mm	9.546 mm
0.584 mm (0.0230 in.)	10.075 mm	9.995 mm
0.610 mm (0.0240 in.)	11.050 mm	11.090 mm

[a] The least squares values were obtained from an unweighted polynomial ($A + Bx + Cx^2$) fit of the theoretical width values.

TABLE II

Experimental Widths of the Collimator's Image at the Surface of the Detector

Experimental Measurement		Experimental Width at Detector's Surface, mm
No. 1		9.19
No. 2		8.99
No. 3		9.31
	Average	9.16 ± 0.13

TABLE III

Gamma Scanning and Radiochemical Quantitative Results for Three (U, Pu) Carbide Sections

Isotope	Gamma Scanning[a, b] (Atoms)[c]	Radiochemical[a] (Atoms)[c]		Difference
^{106}Ru- ^{106}Rh				
	$1.74 \pm 0.04 \times 10^{18}$	$1.80 \pm 0.05 \times 10^{18}$		3.1 %
	$2.08 \pm 0.04 \times 10^{18}$	$2.13 \pm 0.04 \times 10^{18}$		2.6 %
	$1.69 \pm 0.03 \times 10^{18}$	$1.76 \pm 0.06 \times 10^{18}$		3.6 %
			Average	3.1 %
^{137}Cs				
	$5.27 \pm 0.06 \times 10^{19}$	$5.40 \pm 0.06 \times 10^{19}$		2.5 %
	$6.12 \pm 0.06 \times 10^{19}$	$5.80 \pm 0.06 \times 10^{19}$		5.5 %
	$4.89 \pm 0.06 \times 10^{19}$	$4.97 \pm 0.06 \times 10^{19}$		1.6 %
			Average	3.2 %
^{144}Ce- ^{144}Pr				
	$4.66 \pm 0.08 \times 10^{18}$	$4.78 \pm 0.09 \times 10^{18}$		2.5 %
	$5.76 \pm 0.08 \times 10^{18}$	$5.45 \pm 0.08 \times 10^{18}$		5.8 %
	$4.58 \pm 0.08 \times 10^{18}$	$4.58 \pm 0.08 \times 10^{18}$		0.0 %
			Average	2.8 %

[a] The ± value associated with each measurement represents the deviation due to the counting statistics.

[b] Approximately 25 complete gamma-ray spectra were used to obtain the gamma scan data.

[c] The number of atoms was computed using the appropriate half-lives and branching ratios.

TABLE IV

Gamma Scanning and Radiochemical Quantitative Results for Three UO_2-PuO_2 Oxide Sections

Isotope	Gamma Scanning[a, b] (Atoms)[c]	Radiochemical[a] (Atoms)[c]	Difference
^{106}Ru- ^{106}Rh			
	$1.17 \pm 0.03 \times 10^{18}$	$1.12 \pm 0.03 \times 10^{18}$	5.0 %
	$1.34 \pm 0.03 \times 10^{18}$	$9.55 \pm 0.12 \times 10^{17}$	40.1 % (Reject)
	$1.28 \pm 0.03 \times 10^{18}$	$1.25 \pm 0.02 \times 10^{18}$	3.6 %
		Average	4.3 %
^{137}Cs			
	$3.50 \pm 0.04 \times 10^{19}$	$3.61 \pm 0.04 \times 10^{19}$	3.1 %
	$5.68 \pm 0.05 \times 10^{19}$	$5.83 \pm 0.05 \times 10^{19}$	2.8 %
	$4.17 \pm 0.05 \times 10^{19}$	$4.44 \pm 0.05 \times 10^{19}$	6.0 %
		Average	4.0 %
^{144}Ce- ^{144}Pr	$2.34 \pm 0.06 \times 10^{18}$	$2.40 \pm 0.03 \times 10^{18}$	2.8 %
	$2.54 \pm 0.08 \times 10^{18}$	$2.45 \pm 0.03 \times 10^{18}$	3.9 %
	$2.39 \pm 0.08 \times 10^{18}$	$2.44 \pm 0.03 \times 10^{18}$	1.9 %
		Average	2.9 %
^{95}Zr	$1.36 \pm 0.10 \times 10^{16}$	$1.52 \pm 0.03 \times 10^{16}$	10.8 %
	$1.37 \pm 0.07 \times 10^{16}$	$1.49 \pm 0.03 \times 10^{16}$	8.0 %
	$1.28 \pm 0.08 \times 10^{16}$	$1.41 \pm 0.03 \times 10^{16}$	9.1 %
		Average	9.3 %

[a] The ± value associated with each measurement represents the deviation due to the counting statistics.

[b] Approximately 25 complete gamma-ray spectra were used to obtain the gamma scan data.

[c] The number of atoms was computed using the appropriate half-lives and branching ratios.

TABLE V

Relative Burnup Values Determined Using ^{137}Cs as the Fission Monitor

Sample	^{137}Cs Atoms	Number of[a] Fissions	Fissionable Atoms Present	Relative[b] Burnup	Gamma Scanning Normalized[c] Values	Mass Spectrometry Normalized[d] Values
No. 1	5.28×10^{19}	7.17×10^{20}	8.56×10^{21}	9.85 at. %	0.985	0.976
No. 2	6.12×10^{19}	8.33×10^{20}	10.31×10^{21}	9.51 at. %	0.951	0.952
No. 3	4.90×10^{19}	6.66×10^{20}	7.82×10^{21}	10.00 at. %	1.000	1.000

[a] A weighted fission yield of 6.26 % was used to calculate the number of fissions.

[b] The relative burnup is the calculated burnup at the time of measurement. The actual burnup values would be calculated from these values based on the specific decay time. An irradiation period of several years is required for reaching a burnup of 10.0 at. % and ^{137}Cs has a half-life of 30 years, therefore absolute burnup values would be the Relative Burnup values times a decay time correction.

[c] Normalized to the maximum value of 10.0 at. % determined by gamma scanning.

[d] Normalized to the maximum value of 9.84 at. % determined by mass spectrometry.

FIGURE CAPTIONS

Fig. 1 Block diagram of the LASL gamma scanning system.

Fig. 2 Simulated gamma-ray beam image on the surface of the Ge(Li) detector located 1736.6 mm from the source

Fig. 3 The isometric projection of the surface response function for the 661.6 keV gamma-ray energy.

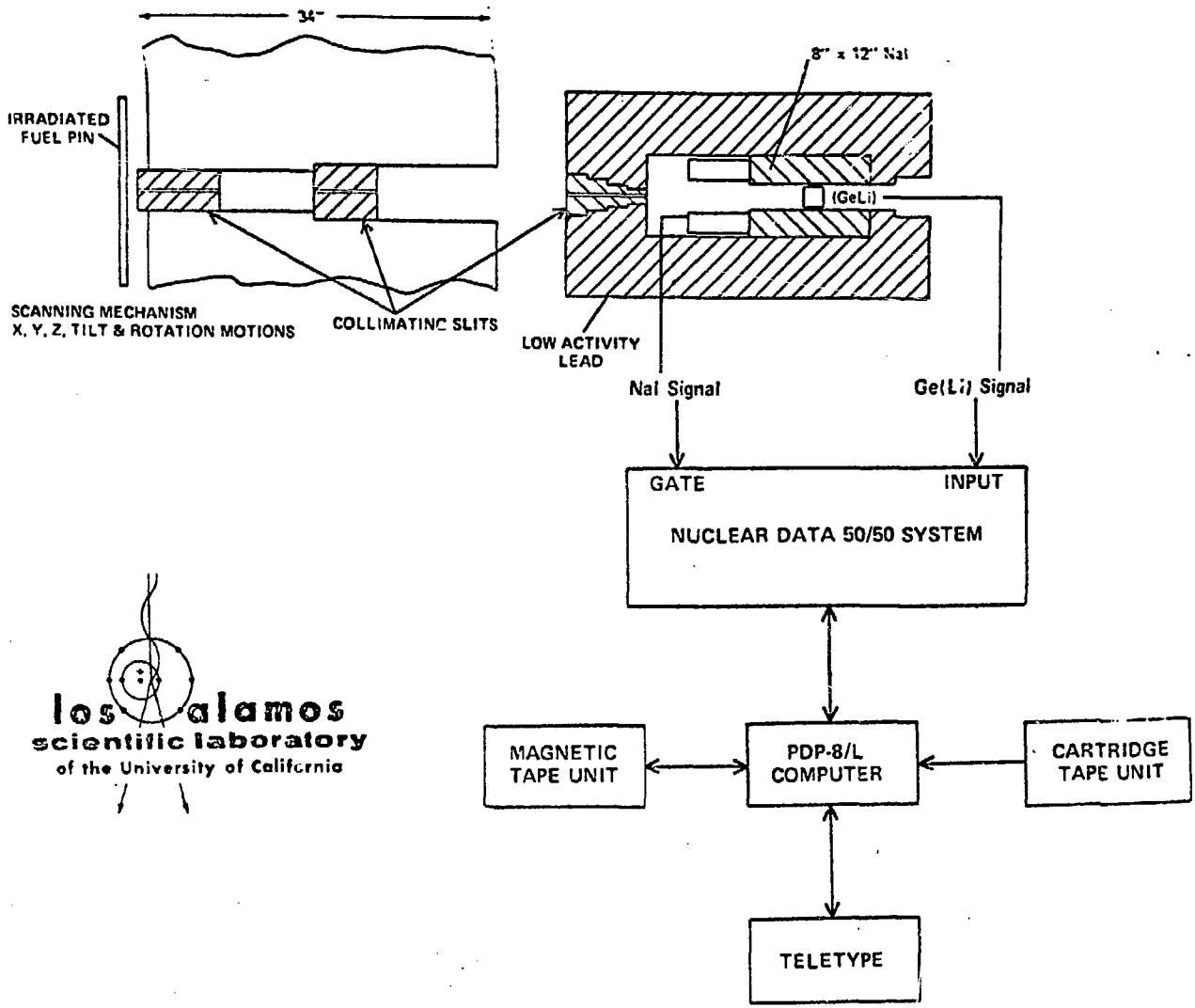

los alamos
scientific laboratory
of the University of California

Simulated Collimator Image on Detector's Surface

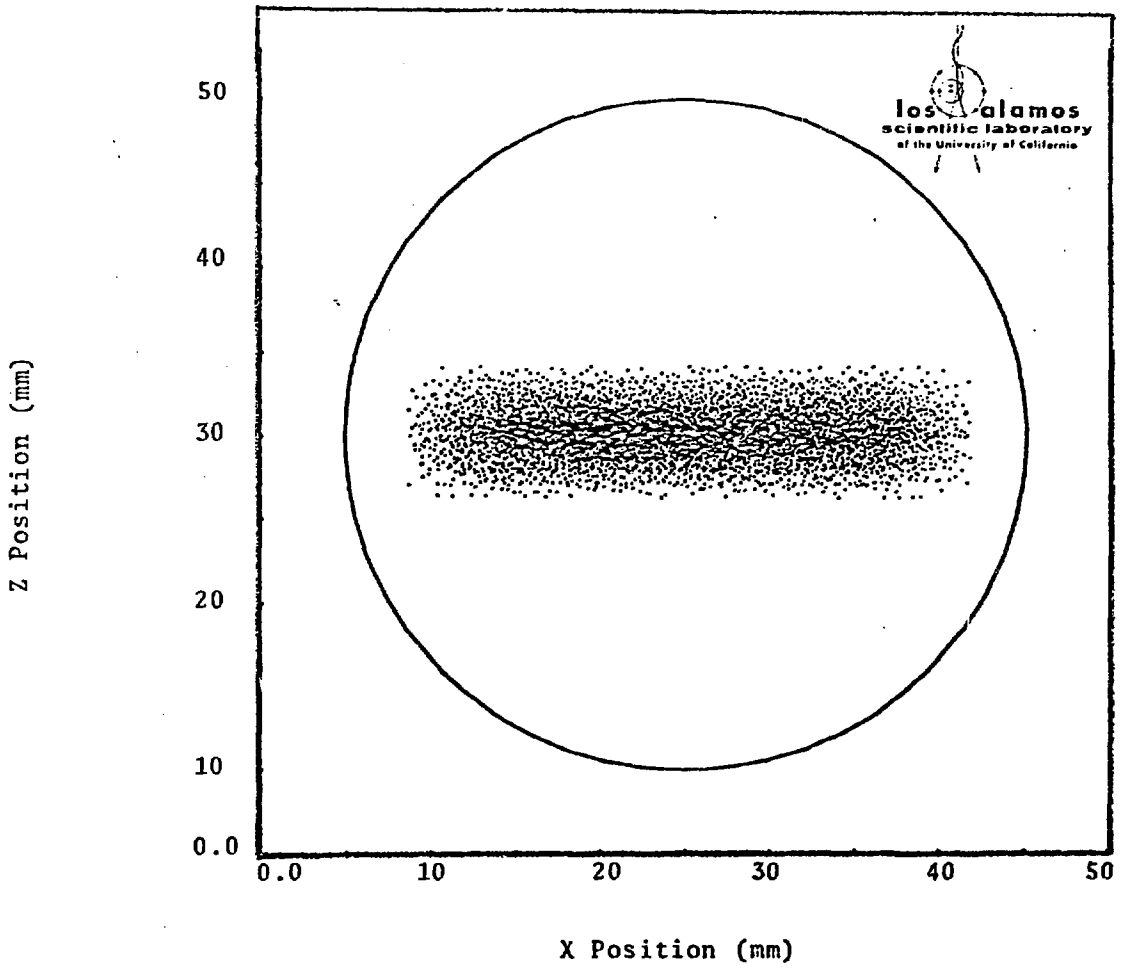
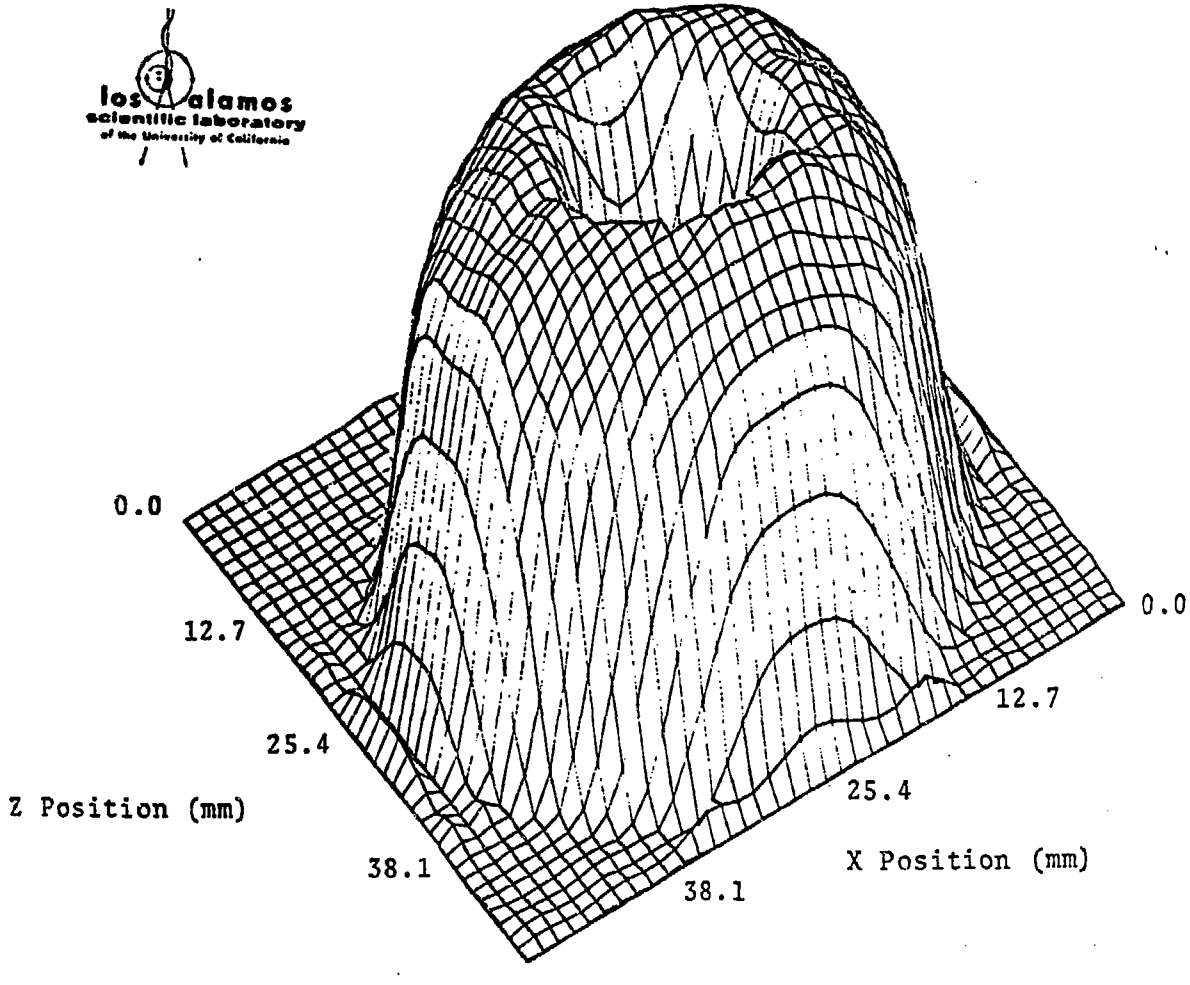
Surface Response Function for 661.6 keV Gamma-ray Energy